ARCHIVES OF CIVIL AND MECHANICAL ENGINEERING 16 (2016) 835–844

Available online at www.sciencedirect.com

ScienceDirect

journal homepage: http://www.elsevier.com/locate/acme

Original Research Article

Soldering aluminium to copper with the use of interlayers deposited by cold spraying

Tomasz Wojdat, Marcin Winnicki *, Małgorzata Rutkowska-Gorczyca, Szymon Krupiński, Krzysztof Kubica*

Wrocław University of Technology, Wyb. Wyspiańskiego 27, 50371 Wrocław, Poland

ARTICLE INFO

Article history:
Received 11 March 2016
Accepted 12 June 2016
Available online 14 July 2016

Keywords:
Cold spray
Soldering
Interlayers
Aluminium coatings
Copper coatings

ABSTRACT

The article presents the application of interlayers deposited by Low Pressure Cold Spraying (LPCS) in the soldering process. The problems concerning soft soldering of aluminium and copper were indicated and a solution with the use of metallic and composite interlayers was proposed. Wettability and spreadability tests with selected solders were performed to evaluate a solderability of various aluminium and copper LPCS coatings. Light and scanning microscopes were used to analyze solder dissimilar Al–Cu joints with previously deposited LPCS interlayer. What is more mechanical properties of the joints, e.g. microhardness and shear strength, were examined. Strength of the soldered Al–Cu joints with the LCPS interlayer highly depend on shape of powder used in spraying process. The joints with the interlayer sprayed with dendritic copper powder have low strength of about 20 MPa. However, the strength of soldered joints with the LPCS interlayer of spherical copper powder is significantly higher and amounts to 36.7 MPa.

1. Introduction

Joints of aluminium with copper are nowadays more and more often applied in different industry branches, e.g. electrical engineering, radio engineering, refrigeration, automotive, aircraft and space industries. However, most of the equipment built with this two dissimilar materials is sensitive to high temperatures. Therefore the low energy welding methods are used for its production [1–3]. The commonly applied welding process is soft soldering, where aluminium is joined to copper with the use of zinc–aluminium solders and the fluxing agents of high chemical activity containing cesium compounds. However, application of Zn–Al solders with high melting point (of about 400 °C) causes formation of the reaction zone at the boundary of the soldered joint and copper. This reaction zones consist of intermetallic phases from the Cu–Zn system and have high microhardness over 500 HV0.025 [4,5]. The identification of phases requires performing the XRD analysis with the X-ray diffraction method. The reaction zone reaches a width up to 50 μm and causes brittleness of soldered joints, what significantly lowers their functionality.

Another problem of soft soldering process is insufficient wettability of copper with the Zn–Al solders (the contact angle $\theta > 50^{\circ}$). Thus the tight filling of the solder gap is problematic [4]. What is more an erosion of the solder joint caused by

* *Corresponding author*. Tel.: +48 713202735; fax: +48 713202735.
E-mail address: marcin.winnicki@pwr.edu.pl (M. Winnicki).

http://dx.doi.org/10.1016/j.acme.2016.06.002

electrochemical corrosion can occur as a result of high potential difference between aluminium and copper.

According to the literature [4], an application of the interlayer deposited on the copper surface in the soldering process is a solution to the described problems. On the one hand deposited interlayer improves copper solderability with zinc solders. On the other hand the interlayer effectively limits creation of the reaction zones. Applied in [4] the Zn–Ni (12–15% Ni) electroplated coating with thickness of 16 μm was used as an interlayer. However, deposition of electroplated coatings is less economical due to the long time of production The time required for depositing the layer of the recommended thickness of 16 μm at the deposition rate of 0.18 μm/min amounted to 1.5 h.

Hence it is necessary to look for another method of depositing the interlayers applied for the soldering process. However, the performed interlayers should: (i) be characterized with good solderability, (ii) provide the effective protection against formation of the hard reaction zones lowering the mechanical properties of joints, and (iii) protect the joint against corrosion.

The newest among thermal spraying methods, e.g. cold spray, provide very good quality of coatings [6,7]. Cold spray can be divided into Low Pressure Cold Spraying – LPCS, and High Pressure Cold Spraying – HPCS. In the LPCS method the pressurized working gas (air or nitrogen) is heated to temperature within the range of 200–650 °C and accelerated to the supersonic velocities in the convergent–divergent de Laval nozzle. The powder particles introduced into the nozzle gain the velocity from the flowing gas as a result of the drag force. Due to the high kinetic energy the particles are plastically deformed at the instant of contact with the substrate and the mechanical bonding occurs. The powder temperature during spraying is much lower than the melting point of the applied metal. Therefore the coating is built in the solid state. Moreover low temperature of the LPCS process decreases coating oxidation compared to the other thermal spraying methods [8–14].

In the article the application of interlayers in the soft soldering of aluminium to copper deposited with the LPCS method has been proposed. In the relevant literature there is little information on the subject [15–17]. The interlayers sprayed with the aluminium powder onto copper substrate, as well as the interlayers sprayed with the copper powder onto aluminium substrate, were subjected to the tests. Evaluation of the coatings solderability was performed based on the spreadability and wettability tests of surfaces using the Zn–Al and Sn–Cu solders. For the selected coatings the soldered joints were performed and analyzed with various tests what is described further in the article.

2. Test methodology

The interlayers were sprayed with the LPCS method using the low-pressure device DYMET 413 (Obninsk Center for Powder Spraying, Obninsk, Russia), equipped with a spraying gun and the de Laval nozzle of the 5 mm output diameter. The spraying gun was attached to the manipulator operating in 3 axes: x, y and z. The air was used as a working gas with pressure of 0.9 MPa and temperature of 200 °C and 600 °C for aluminium and copper powders, respectively. The remaining parameters of the process: (a) the powder feed rate of 40 g/min, (b) the traverse speed of 10 mm/s, and (c) the spray distance of 10 mm.

The coatings were deposited using commercially available powders: (i) gas atomized aluminium (Al) with particle size of −63 + 10 μm (PyroGarage, Poland) (Fig. 1a), (ii) aluminium mixed with alumina (Al + Al_2O_3) with particle size of −45 + 5 μm (Obninsk Center for Powder Spraying, Russia) (Fig. 1b), (iii) electrolytic copper (E-Cu) with particle size of −50 + 15 μm (Libra Ltd., Poland) (Fig. 1c), (iv) copper mixed with alumina (E-Cu + Al_2O_3) with particle size of −45 + 15 μm (Obninsk Center for Powder Spraying, Russia) (Fig. 1d), (v) gas atomized copper (S-Cu) with particle size of −55 + 10 μm (Sentes-BIR A.S., Turkey) (Fig. 1e), (vi) copper mixed with alumina (S-Cu + Al_2O_3) with particle size of −50 + 10 μm (Sentes-BIR A.S., Turkey) (Fig. 1f). The metallic powders were mixed with alumina in the weight ratio 1:1. Addition of alumina was applied to increase the density, adhesion and reduce porosity of the coatings. The aluminium coatings were deposited on the copper substrate of the Cu-ETP grade, and the copper coatings on the aluminium substrate of the AA1350 grade. The substrates were in the form of squares of the 30 mm × 30 mm size and 2 mm thick. Prior to spraying the substrates were degreased and sand blasted using alumina (mesh 20).

Prior to the tests the coatings were grinded with papers of: 80, 200, 400, 600, 800 and 1000 grade, to remove the waviness and roughness created during the spraying process.

For evaluation of solderability of the Al coatings deposited onto the copper substrates the near-eutectic zinc solder S-ZnAl4 (Al – 4 wt.%) was used, with the melting point in the range of 382–387 °C, and the 192 NX flux, containing cesium compounds. In the case of Cu coatings deposited onto aluminium substrates the tin solder S-SnCu3 (Cu – 3 wt.%) was used, with melting point in the range of 230–250 °C and a flux containing zinc chloride and ammonium chloride. The same solders and fluxes were also applied in soft soldering process of dissimilar materials with deposited interlayers.

The specimens with deposited coatings and the proper solders of the 0.1 g and the fluxes of the 0.05 g on the surface, were placed on a metal mesh coated with ceramics. Afterwards the specimens were heated from the bottom with the propane-air flame using the Bunsen burner. Since melting of the solder the specimens were heated for 5 s.

The solderability was determined by examination of solder spreadability and wettability. The measure of spreadability was the size of the solder spread area at a given substrate. Therefore the DP-Soft optical program was used to measure soldered area. The wettability was determined by measuring of the contact angle θ. Therefore the specimens were cut in the half of the spread solder and metallographic sections were analyzed. Finally the contact angles for individual coatings were obtained by image analysis.

For the strength tests the overlap joints were prepared with the overlap length of 5 mm. Width of the soldering gap of 0.2 mm was fixed with the steel distance wires. The joints were made by heating with the propane-air flame. The static shearing test was performed at the Instron 3369 testing machine, using the handle with spacing inserts. The traverse speed of the machine was 0.2 cm/min, and the range of loads up to 50 kN.

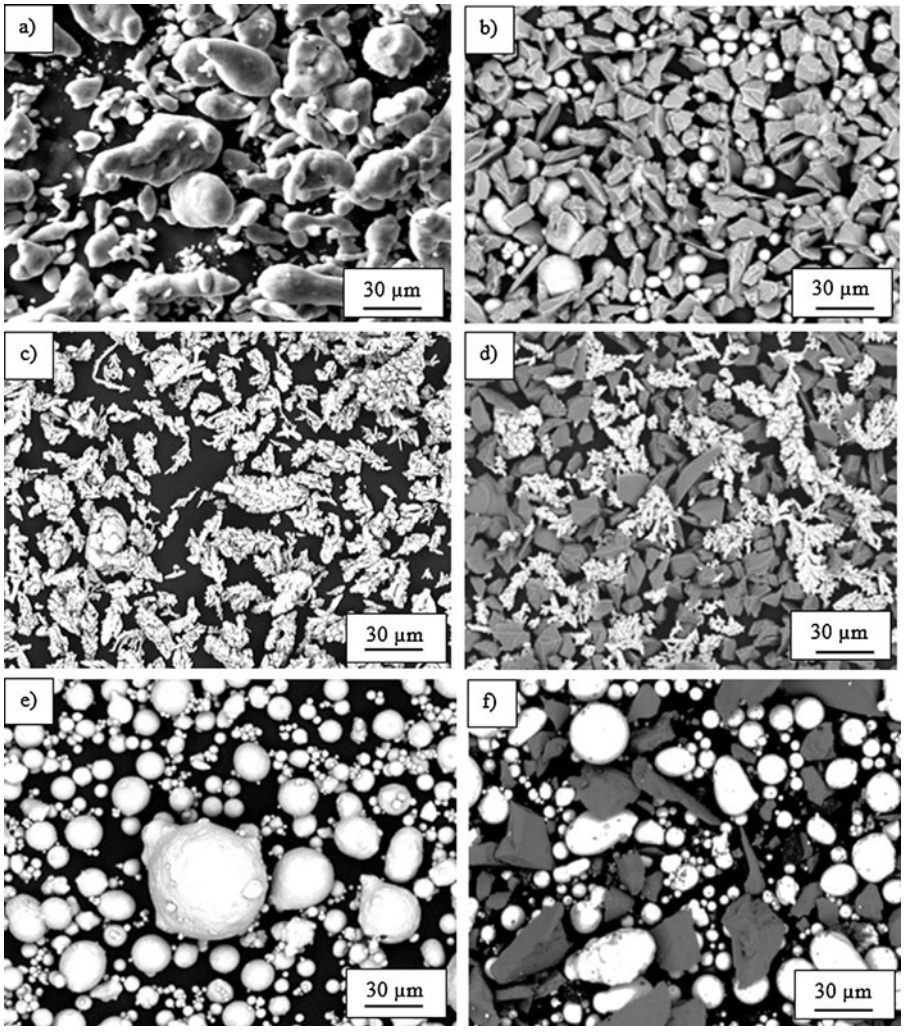

Fig. 1 – The powders used in the tests: Al (a), Al + Al_2O_3 (b), E-Cu (c), E-Cu + Al_2O_3 (d), S-Cu (e), S-Cu + Al_2O_3 (f). SEM, BSE.

The soldered specimens for metallographic tests and microhardness measurements were prepared with the overlap length of 10 mm to ensure better analysis. The metallographic specimens were grinded on water abrasive papers of up to 2000 grade, and polished with aluminium oxide. The cross-sections were observed using the light and scanning microscopes, Nikon Eclipse MA200 and Phenom G2, respectively. The microhardness was measured with the Vickers method, in accordance with the ISO 6507 standard, using the digital hardness testing machine Micro Vickers HVS-1000, with the force of 0.25 N. The measurements of microhardness were performed along the four measuring lines: (i) two vertical lines passing through all zones of the joint, (ii) a horizontal line in the soldered joint and (iii) a horizontal line in the interlayer.

3. Results and discussion

3.1. *Microstructure of the coatings*

Microstructure of coatings deposited with the LPCS methods is shown in Fig. 2. The coatings thickness was in the range of 250–300 μm. The coatings deposited using the copper dendritic powder (Fig. 2c) had visible porosity. Admixture of ceramics to the powder led to intensive work hardening of metal particles, what increased density of the coating (Fig. 2d). In the case of spherical powder of aluminium and copper the metallic coating showed high density (Fig. 2a, e), and admixture of alumina resulted in additional reinforcement (Fig. 2b, f).

Table 1 presents average roughness of the coating surfaces after the grinding process. The arithmetic mean surface roughness *Ra* of coatings was in the range of 0.2–0.34 μm. Only the E-Cu coating showed significantly higher *Ra* roughness of 13.2 μm, as a result of non-uniform deposition and high porosity. What is more total height of the roughness profile *Rt* was also considerably higher in the case of E-Cu coating.

3.2. *Spreadability and wettability*

Evaluation of solderability of the Al and Cu coatings was performed at the base of solder spreadability and wettability tests. The exemplary spread area of the S-ZnAl4 solder on the Cu-ETP substrate with the deposited Al and Al + Al_2O_3 coatings are shown in Fig. 3.

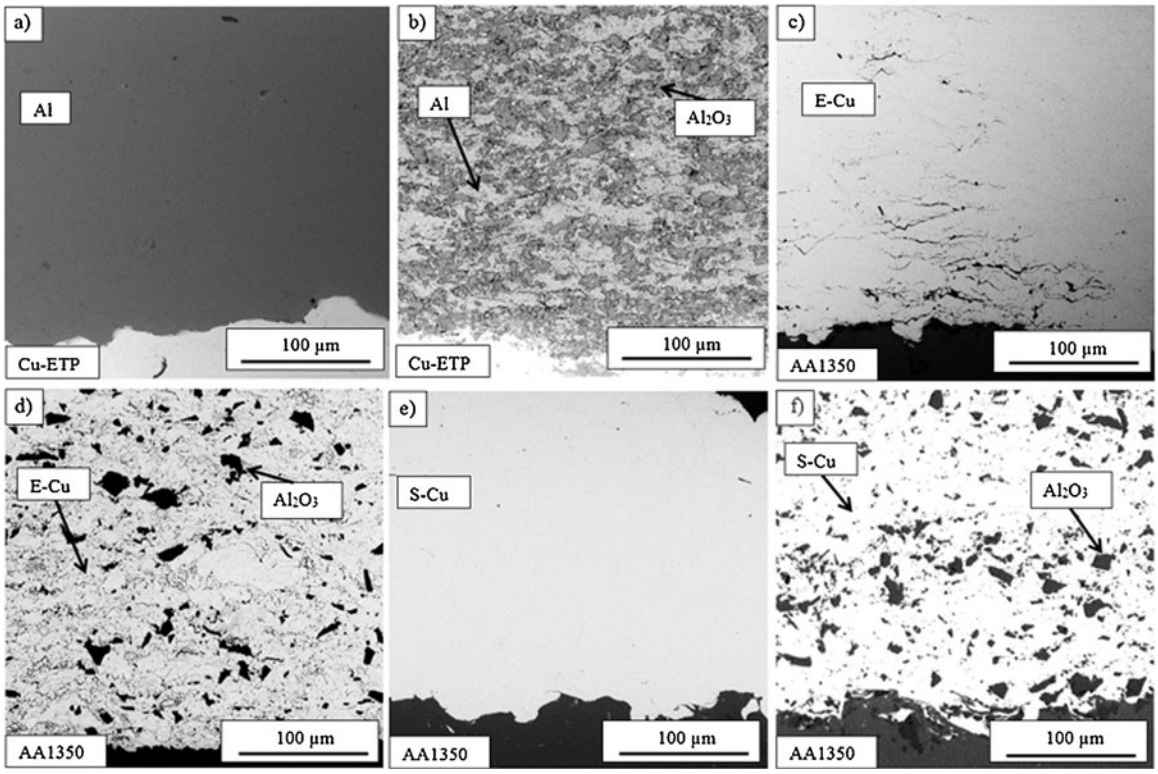

Fig. 2 – Microstructure of LPCS coatings: Al (a), Al + Al_2O_3 (b), E-Cu (c), E-Cu + Al_2O_3 (d), S-Cu (e) and S-Cu + Al_2O_3 (f). SEM, BSE.

Table 1 – Average roughness of LCPS coatings.

No.	Coating	Ra [µm]	Rt [µm]
1.	Al	0.33	5.38
2.	Al + Al_2O_3	0.24	7.23
3.	E-Cu	13.2	105.2
4.	E-Cu + Al_2O_3	0.22	2.84
5.	S-Cu	0.20	7.42
6.	S-Cu + Al_2O_3	0.34	8.91

The spreadability of the S-ZnAl4 solder on the copper substrate with the Al coating was very good, the average value of five measurements of spread solder areas was 410 mm^2 (Fig. 3a). This is almost twice higher than spreadability of the S-ZnAl4 solder on the surface of AA-1050A aluminium alloy [18]. However, on copper substrates with deposited Al + Al_2O_3 coating the S-ZnAl4 solder was not spreading at all (Fig. 3b), each time a ball of solder not wetting its surface was created at the specimen. Presence of the Al_2O_3 particles in the coating disabled spreading of the solder. The chemically active flux

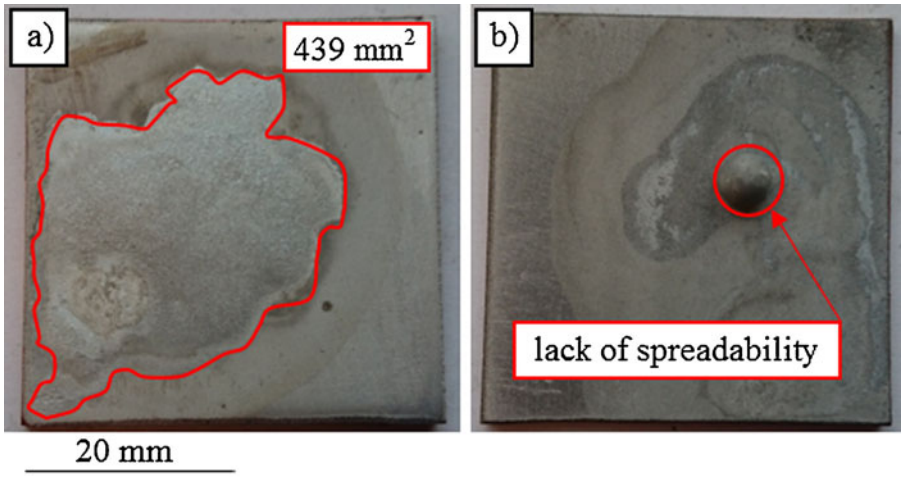

Fig. 3 – Spreadability of the S-$ZnAl_4$ solder at the Cu-ETP substrate with the deposited Al coating (a) and lack of spreadability of the L-$ZnAl_4$ solder at the Cu-ETP substrate with the deposited Al + Al_2O_3 coating (b).

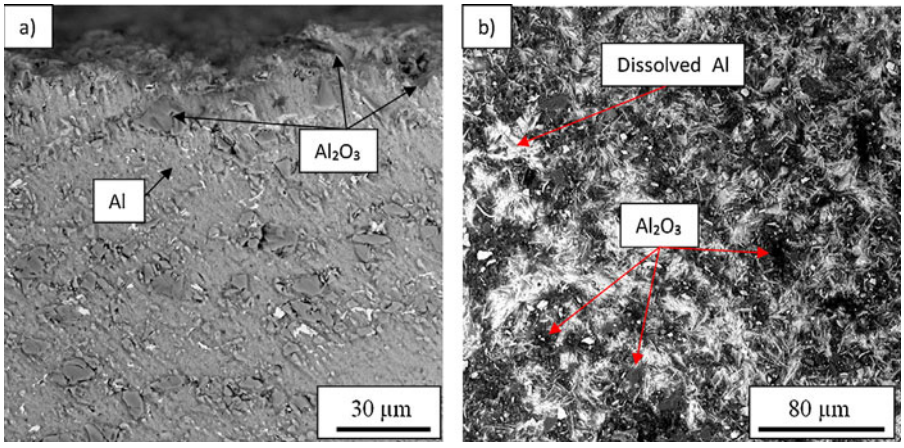

Fig. 4 – Microstructure of Al + Al_2O_3 coating with dissolved by fluxing agent Al matrix, top part (a) and surface (b). SEM, BSE.

dissolved the Al matrix, leaving the protruding particles of alumina, which are hardly wetted by the solder (Fig. 4). For this reason in further part of the study the Al + Al_2O_3 coatings were not tested.

Table 2 presents average value of spread areas for the S-SnCu3 solder on the AA1350 substrate with the E-Cu, S-Cu, E-Cu + Al_2O_3 and S-Cu + Al_2O_3 coatings. Fig. 5 shows the exemplary spreadability surfaces.

The obtained results showed highest spreadability of the S-SnCu3 solder on the coating sprayed with a dendritic copper powder (E-Cu). The solder spreadability on coating sprayed with a spherical copper powder is considerably lower. It arises probably from the difference in oxidation level of the copper powders prior to spraying [21–23]. What is more the solder spreadability on composite coatings decreases of about 50%.

The results of contact angle measurements for individual coatings are presented in Table 3. An exemplary specimens with the Al and E-Cu coatings prepared for measurements of contact angle are shown in Fig. 6.

The average value of the contact angle of the Al coating amounted to 2°. Thus Al coating showed very good wettability with the Zn–Al solder. The surface of Al coating deposited on the copper substrate was dissolved as a result of high chemical activity of the flux (Fig. 6a). However the thickness of the dissolved material depends mostly on the heating time, which is measured since the flux transition from the solidus state into the liquidus state. In case of spreadability and wettability tests the time was 5 s, and the thickness of dissolved material was in the range of 14–20 μm.

The wettability of aluminium coating with Zn–Al solder is higher compared to the wettability of copper coatings with Sn–Cu solder. The value of contact angle amounted to 15° and 35° for coatings sprayed with dendritic metallic E-Cu and composite E-Cu + Al_2O_3 powders, respectively. Moreover, for the coatings sprayed with spherical metallic S-Cu and composite S-Cu + Al_2O_3 powders the average value of contact angle amounted to 23° and 38°, respectively. However, all obtained results are much better compared to the wettability of copper with the Zn-Al solders, where contact angle is above 50° [4].

It should be noted that the contact angle up to 30° confirms good wettability of the material. Thus coatings sprayed with all metallic powders have good solderability and may be used as interlayers for soldering aluminium with copper. Therefore the overlap joints were performed only with the use of the Al, E-Cu and S-Cu powders. However the contact angle of copper composite coatings is not large enough to disqualify the use of those coatings for soldering.

Table 2 – Spreadability of the S-$SnCu_3$ solder on the AA1350 substrate with the deposited copper coatings.

No.	Coating	Solder	Spreadability [mm^2]
1.	E-Cu	S-$SnCu_3$	122
2.	E-Cu + Al_2O_3		78
3.	S-Cu		90
4.	S-Cu + Al_2O_3		58

3.3. *Mechanical properties of the soldered joints*

The static shearing test was used to evaluate mechanical properties of soldered joints of aluminium with copper with the interlayers deposited by the LCPS method. Three types of overlap joints were prepared for the test – joints with interlayer of Al, soldered with application of the S-ZnAl4 solder and joints with interlayer of E-Cu and S-Cu soldered with application of the S-SnCu3 solder. The obtained results from five measurements for each joint type are present in Table 4.

The shear strength of Al–Cu soldered joints with interlayer sprayed with metal powders of Al and E-Cu was about 20 MPa. Much higher results of 36.7 MPa were obtained for joints soldered with interlayer sprayed with spherical copper powder. To analyze such significant differences in strength of individual types of joints the evaluation of the failure mechanisms was performed on the base of fractures after the static shear test. Fig. 7 presents exemplary fractures of the specimens after the shear tests for each type of joint.

The obtained results showed that low mechanical strength of the Al–Cu joints with Al interlayer was a result of weak adhesion of the deposited coating on the copper substrate. The

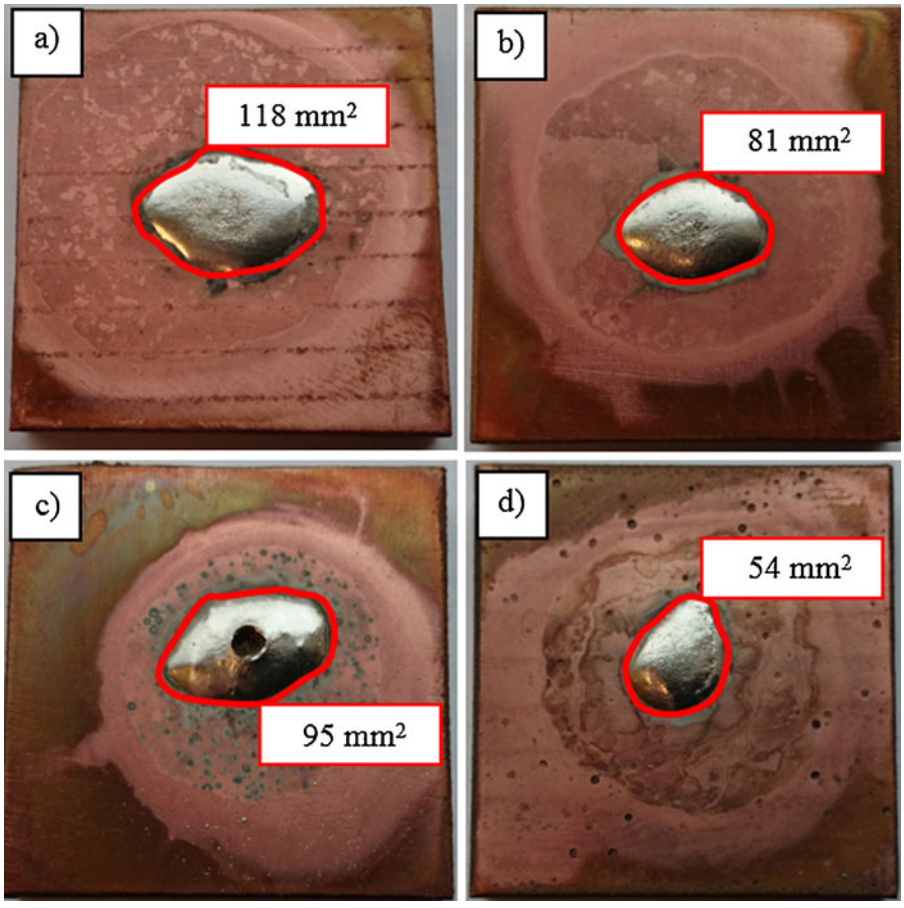

Fig. 5 – Spreadability of the S-SnCu3 solder on the AA1350 substrate with the E-Cu (a), E-Cu + Al_2O_3 (b), S-Cu (c) and S-Cu + Al_2O_3 coatings.

Table 3 – Results of contact angle measurements.

No.	Coating	Solder	Contact angle
1.	Al	S-$ZnAl_4$	2°
2.	E-Cu	S-$SnCu_3$	15°
3.	E-Cu + Al_2O_3		35°
4.	S-Cu		23°
5.	S-Cu + Al_2O_3		38°

mechanism of the fracture is adhesive. Fig. 7a clearly shows the LPCS interlayer detached from the Cu-ETP substrate all over the surface. This demonstrates the high cohesion within the coating and the low adhesion between the coating and the substrate.

On the other hand the low strength of the Al–Cu joints with the E-Cu interlayer results from low cohesion forces in the

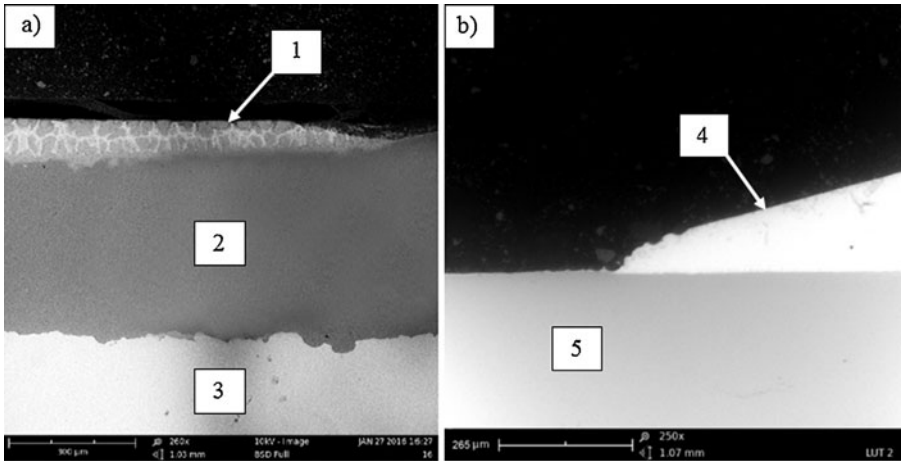

Fig. 6 – The specimens prepared for measurements of contact angles, Al (a) and E-Cu (b) coatings; 1 – S-ZnAl4, 2 – Al, 3 – Cu-ETP, 4 – S-SnCu3, 5 – E-Cu.

Table 4 – The shear strength of the aluminium and copper soldered joints with the LCPS interlayers.

No.	Coating	Solder	Shear strength [MPa]
1.	Al	S-ZnAl4	20.9
2.	E-Cu	S-SnCu3	22.9
3.	S-Cu		36.7

coating. Thus failure of the specimen was the effect of decohesion in the E-Cu interlayer (Fig. 7b). The low cohesion within the coating may result from high porosity (see Fig. 2c).

In case of joints with the S-Cu interlayer the failure occurred in the soldered joint as a result of decohesion (Fig. 7c). Therefore the continuous layer of the solder remained on both parts of the specimen. Thus the maximum strength for the soldered joint was reached. To increase the shear strength of the joint a solder with better mechanical properties should be used. The spherical shape of the copper powder decreased porosity of the deposited coating and therefore the coating had better mechanical properties [11,12].

The soldered joints with Al and Cu interlayers showed significant difference in microhardness. In the Al–Cu joint soldered with the use of S-ZnAl4 solder the highest microhardness was obtained in the soldered joint and amounted to 95.4 HV0.025. The microhardness of the Al coating was 28.7 HV0.025. On the other hand, the Al–Cu joints soldered with the use of the S-SnCu3 solder showed microhardness of 13.2 HV0.025. The higher microhardness of 92.1 HV0.025 and 163.2 HV0.025 was obtained in E-Cu and S-Cu interlayers, respectively. Spherical powder deforms more intensively in spraying process causing significant increase of hardness of the deposited coating [11,12]. Moreover the increased hardness is caused by impingement effect, which is the hammering of particles on top of each other [14,24].

It is worth stressing that none of the performed joints showed the significant increase in microhardness to the value above 350 HV0.025, what could indicate the formation of the reaction zones [4,19].

3.4. *Metallographic tests*

Macrostructure of the performed overlap joints of the Al–Cu with the deposited interlayers are presented in Fig. 8. Macrostructure of the Al–Cu joint with Al coating revealed the presence of gas bubbles in some locations of the soldered joint and the dissolution of aluminium surface by the S-ZnAl4

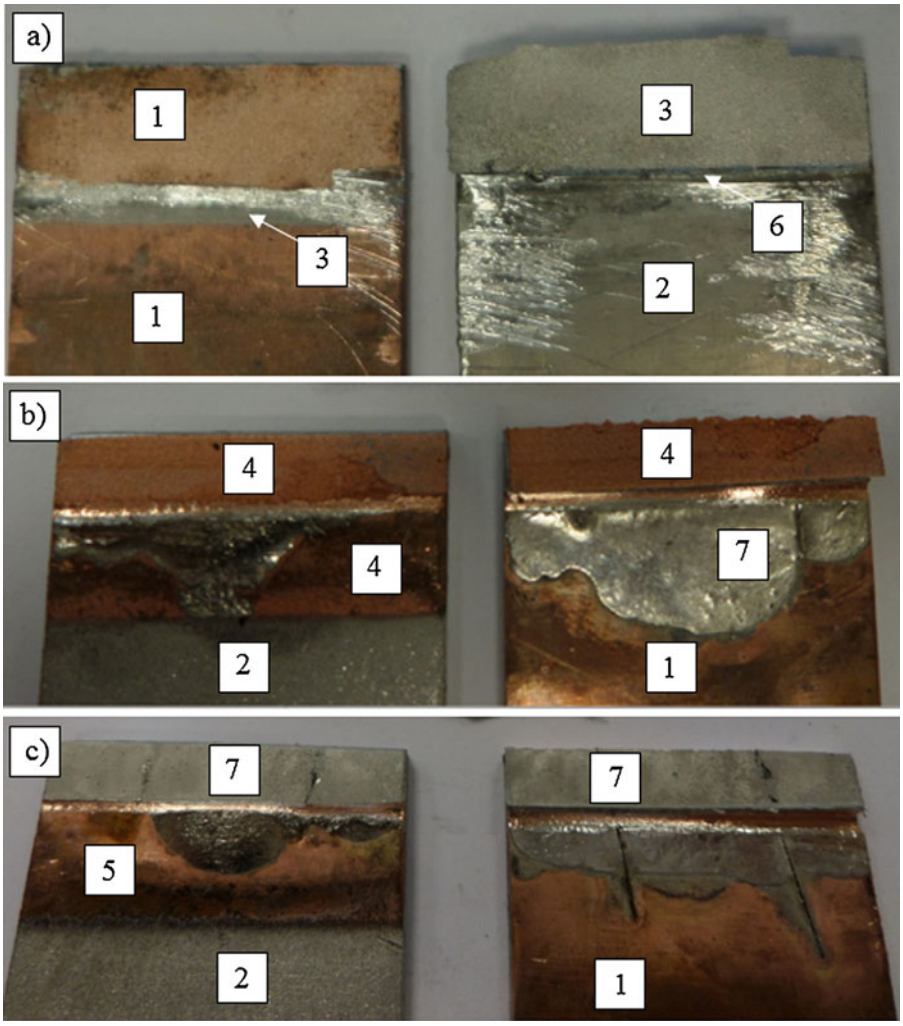

Fig. 7 – Fractures after the shear tests of the Al–Cu joints with the Al (a), E-Cu (b) and S-Cu (c) interlayer. 1 – Cu-ETP, 2 – AA1350, 3 – layer of Al, 4 – layer of E-Cu, 5 – layer of S-Cu, 6 – S-ZnAl4, 7 – S-SnCu3.

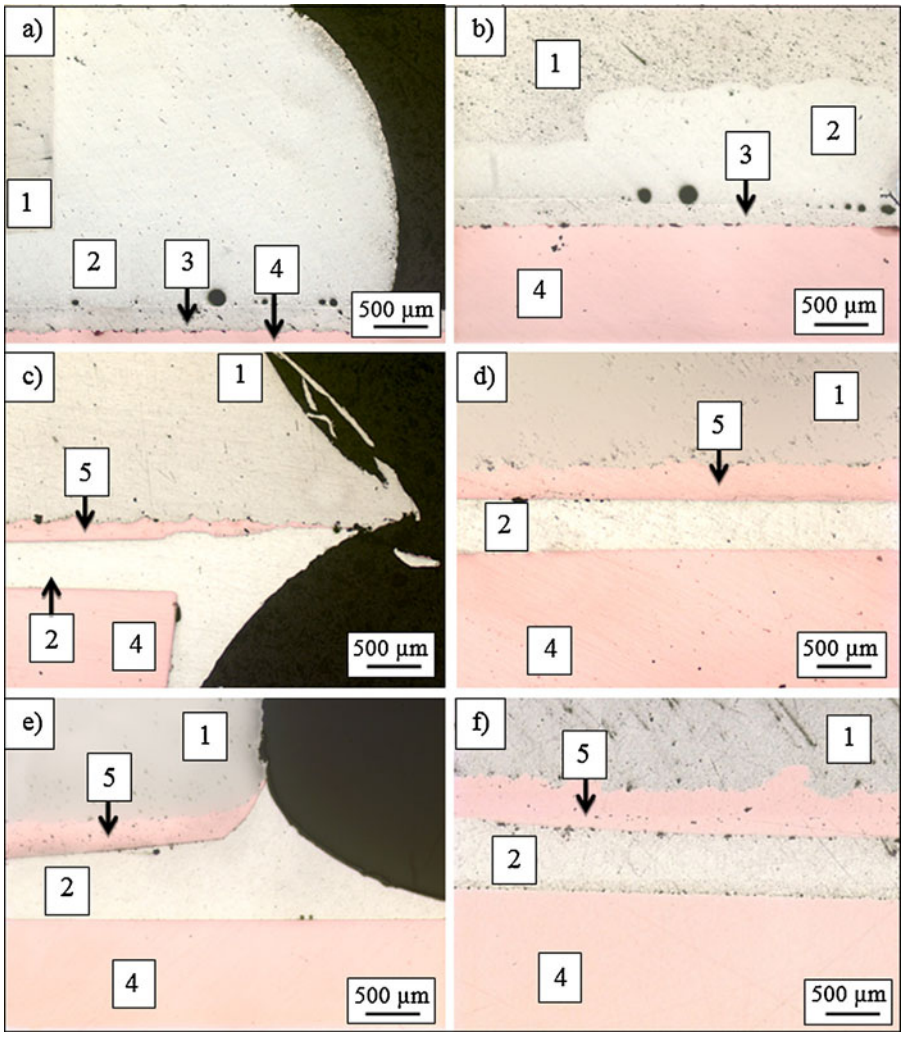

Fig. 8 – Macrostructure of the overlap joint of the Al–Cu with the interlayer: Al (a, b), E-Cu (c, d) and S-Cu (e, f); 1 – Al specimen, 2 – soldered joint, 3 – Al coating, 4 – Cu specimen, 5 – Cu coating.

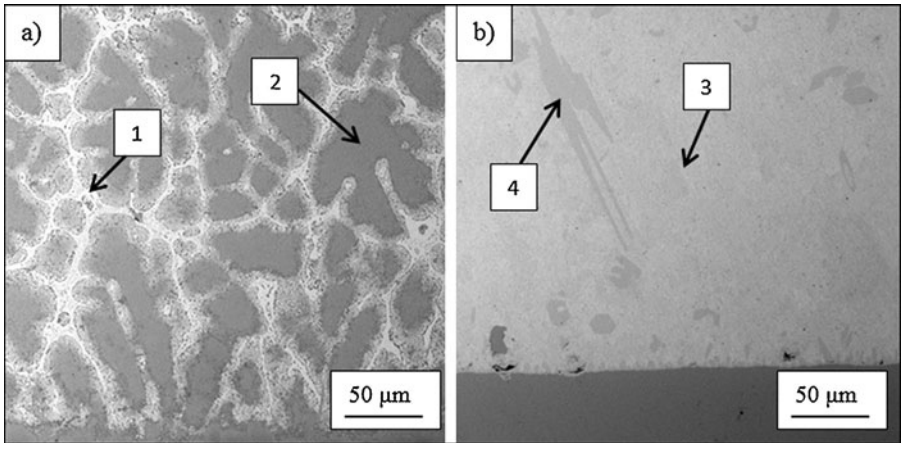

Fig. 9 – Microstructure of the S-ZnAl4 joint (a) and the S-SnCu3 (b) in the overlap joint of the Al–Cu type with the interlayer, 1 – the solid solution η, 2 – ($\eta + \alpha$) eutectics, 3 – (Sn + Cu_6Sn_5) eutectics, 4 – the secondary solid solution Cu_6Sn_5 (SEM, BSE).

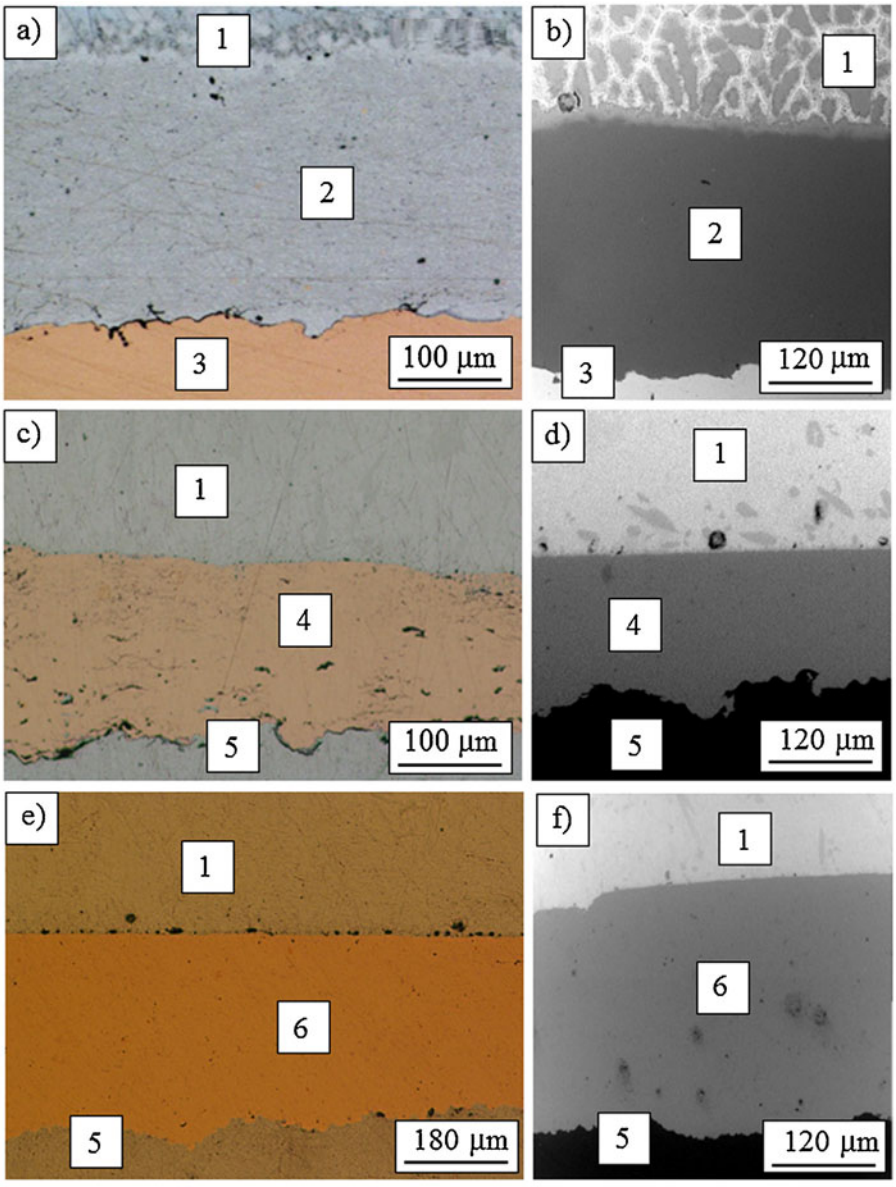

Fig. 10 – Lack of reaction zones at the boundary of interlayer with the soldered joint and the specimen: LM (a, c, e) SEM, BSE (b, d, f), 1 – soldered joint, 2 – Al coating, 3 – Cu specimen, 4 – E-Cu coating, 5 – Al specimen, 6 – S-Cu coating.

solder (Fig. 8b). What is more the soldering defects in the form of gas bubbles appeared also in the Al–Cu solder joints with the E-Cu and S-Cu coatings (Fig. 8d). However joints obtained with cold spray interlayers are very satisfactory compared to the joints made with flame or arc spray interlayers [20].

Microstructure of the joints is shown in Fig. 9. The S-ZnAl4 solder structure (Fig. 9a) showed the dendrites of $(\eta + \alpha)$ eutectics, as well as the solid solution η distributed in the inter-dendritic spaces. The structure of the S-SnCu3 solder (Fig. 9b) consisted of the primary solid solution, which is the $(Sn + Cu_6Sn_5)$ eutectics, and the secondary solid solution Cu_6Sn_5 in the form of darker, irregular phase.

The studies of microstructure showed lack of reaction zones at the interface between solder and interlayers of Al, E-Cu and S-Cu (Fig. 10). What is more, the boundary of interlayers and substrates was also free of reaction zones, which could be created in the soldering process (Fig. 10a, c, e). Thus, it can be concluded, that there were no diffusion phenomena, and bonding of the individual interlayers both, with the substrate and with the soldered joint, is adhesive.

4. Conclusions

Based on the obtained results, the following conclusions were drawn:

- The coatings deposited with the LPCS method had good soldering properties, and thus can be used as interlayers in the soldering processes.
- Addition of alumina to Cu powder caused decrease of soldering properties of the deposited composite coating and

in case of the Al powder significantly limited the wettability of the composite coating with Zn–Al solder, what eliminated the use of Al + Al_2O_3 powder in the soldering process.
- Shape of the powder (dendritic, spherical) used in spraying influenced the porosity and roughness of the coating, and thus soldering properties of the deposited coating as well. The coatings sprayed of the dendritic powder had better wettability and spreadability with Sn–Cu solder.
- The interlayers deposited with the LCPS method effectively limited formation of the reaction zones at the boundary of the coating with the soldered joint.
- The coatings deposited of the spherical copper powder (S-Cu) had the highest mechanical properties compared to the other powder used and thus were attractive for soldering processes.

REFERENCES

[1] H.M. Howard, Solders and Soldering, McGraw Hill Professional, 2001. p. 519.
[2] A. Rahn, The Basics of Soldering, Wiley, 1993. p. 369.
[3] M. Pecht, Soldering Processes and Equipment, John Wiley & Sons, 1993. p. 296.
[4] Z. Mirski, T. Wojdat, M. Stachowicz, Soldering of aluminium with copper and steel using intermediate layer Zn–Ni, Archives of Civil and Mechanical Engineering 15 (4) (2015) 903–910.
[5] T.B. Massalski, Binary alloys phase diagrams, ASM International 1 (1992).
[6] L. Pawłowski, The Science and Engineering of Thermal Spray Coatings, John Wiley & Sons Ltd, New York, 2008.
[7] J. Davis, Handbook of Thermal Spray Technology, ASM International, United States of America, 2004.
[8] F. Gärtner, T. Stoltenhoff, J. Voyer, H. Kreye, S. Riekehr, M. Kocak, Mechanical properties of cold-sprayed and thermally sprayed copper coatings, Surface and Coatings Technology 200 (2006) 770–782.
[9] V.K. Champagne, The Cold Spray Materials Deposition Process – Fundamentals and Applications, Woodhead Publishing Limited, Cambridge, 2007.
[10] R.G. Maev, V. Leshchynsky, Introduction to Low Pressure Gas Dynamic Spray, Wiley-VCH Verlag GmbH & Co, KGaA, Weinheim, 2008.
[11] H. Koivuluoto, P. Vuoristo, Effect of powder type and composition on structure and mechanical properties of Cu + Al_2O_3 coatings prepared by using low-pressure cold spray process, Journal of Thermal Spray Technology 19 (5) (2010) 1081–1092.
[12] H. Assadi, F. Gärtner, T. Stoltenhoff, H. Kreye, Bonding mechanism in cold gas spraying, Acta Materialia 51 (2003) 4379–4394.
[13] H. Koivuluoto, J. Lagerbom, M. Kylmalahti, P. Vuoristo, Microstructure and mechanical properties of low-pressure cold-sprayed (LPCS) coatings, Journal of Thermal Spray Technology 17 (2008) 721–727.
[14] K. Spencer, D.M. Fabijanic, M.-X. Zhang, The use of Al-Al_2O_3 cold spray coatings to improve the surface properties of magnesium alloys, Surface & Coatings Technology 204 (2009) 336–344.
[15] J.F. Li, P.A. Agyakwa, C.M. Johnson, D. Zhang, T. Hussain, D.G. McCartney, Characterization and solderability of cold sprayed Sn–Cu coatings on Al and Cu substrates, Surface and Coating Technology 204 (2010) 1395–1404.
[16] B. Wielage, A. Wank, Th. Grund, Thermally sprayed solder/braze filler alloys for the joining of light metals, in: XII Workshop Plasmatechnik, Ilmenau, September 23–24, 2004.
[17] P.C. King, S.H. Zahiri, M. Jahedi, J. Friend, Cold spray electroding of piezoelectric ceramic, Materials Forum 31 (2007) 116–119.
[18] Z. Mirski, T. Wojdat, Soldered joints aluminium with cupper, non alloy and alloy steel made of zinc binders, Przegląd Spawalnictwa (4) (2013) 2–8.
[19] Z. Mirski, K. Granat, A. Prasałek, The diffusive barriers in copper brazing with austenitic steel by use the Cu–Ag–P (L-Ag15P) filler metal, The Archives Metallurgy and Materials 53 (4) (2008) 1035–1046.
[20] B. Wielage, A. Wank, T.H. Grund, Thermally sprayed solder/braze filler alloys for the joining of light metals, in: The XII Workshop Plasmatechnik, Ilmenau, 23–24 September, 2004.
[21] Ch.-J. Li, W.-Y. Li, H. Liao, Examination of the critical velocity for deposition of particles in cold spraying, Journal of Thermal Spray Technology 15 (2) (2006) 212–222.
[22] Ch.-J. Li, H.-T. Wang, Q. Zhang, G.-J. Yang, W.-Y. Li, H. Liao, Influence of spray materials and their surface oxidation on the critical velocity in cold spraying, Journal of Thermal Spray Technology 19 (1–2) (2010) 95–101.
[23] H. Assadi, T. Schmidt, H. Richter, J.-O. Kliemann, K. Binder, F. Gärtner, T. Klassen, H. Kreye, On parameter selection in cold spraying, Journal of Thermal Spray Technology 20 (6) (2011) 1161–1176.
[24] K.J. Hodder, H. Izadi, A.G. Mcdonald, A.P. Gerlich, Fabrication of aluminum–alumina metal matrix composites via cold gas dynamic spraying at low pressure followed by friction stir processing, Materials Science & Engineering A 556 (2012) 114–121.